

Stark Tuning of Donor Electron Spins in Silicon

F. R. Bradbury,^{1,*} A. M. Tyryshkin,¹ Guillaume Sabouret,¹ Jeff Bokor,^{2,3} Thomas Schenkel,² and S. A. Lyon¹

¹*Department of Electrical Engineering, Princeton University, Princeton, New Jersey 08544, USA*

²*E. O. Lawrence Berkeley National Laboratory, Berkeley, California 94720, USA*

³*Department of Electrical Engineering and Computer Science, University of California, Berkeley, California 94720, USA*

(Received 23 March 2006; published 25 October 2006)

We report Stark shift measurements for ¹²¹Sb donor electron spins in silicon using pulsed electron spin resonance. Interdigitated metal gates on a Sb-implanted ²⁸Si epilayer are used to apply the electric fields. Two quadratic Stark effects are resolved: a decrease of the hyperfine coupling between electron and nuclear spins of the donor and a decrease in electron Zeeman g factor. The hyperfine term prevails at magnetic fields of 0.35 T, while the g factor term is expected to dominate at higher magnetic fields. We discuss the results in the context of the Kane model quantum computer.

DOI: [10.1103/PhysRevLett.97.176404](https://doi.org/10.1103/PhysRevLett.97.176404)

PACS numbers: 71.70.Ej, 03.67.Lx, 71.55.Cn, 76.30.-v

Since Kane's original proposal in 1998 [1], the promise of implementing quantum computation (QC) with spin qubits in silicon has generated much excitement. Recent scaling strategies [2] take advantage of long coherence times of electron [3,4] and nuclear [5] spins and mature silicon technologies. In donor spin QC architectures impurities are arranged in large ordered arrays on the silicon chip, placed in a strong magnetic field, and manipulated by resonant microwave pulses. To operate on single spins in a tightly packed qubit array, it has been suggested that the magnetic resonance be electrostatically tuned (Stark tuning) into and out of resonance with globally applied radio frequency or microwave fields by nanoscopic addressing gates near each donor site.

In this Letter we lay the experimental foundation for these Stark tuning techniques by measuring electrostatic tuning of the spin resonance frequencies of electrons bound to antimony donors in silicon using pulsed electron spin resonance (ESR). The spin resonance Stark shift of the donor electron has been theoretically studied in the context of decreasing the hyperfine interaction with the donor nuclei [6,7]. Applying an external electric field pulls the electron wave function away from the donor nucleus, reducing the hyperfine coupling. In addition to the hyperfine Stark shift, the electron g factor may also change due to admixing with higher orbital hydrogenic states. This g factor change is referred to here as the spin-orbit Stark shift. Our results resolve quadratic hyperfine and spin-orbit Stark effects and thereby provide proof of concept for Stark tuning a qubit's spin resonance.

The donor electron spin in silicon, $S = 1/2$, is coupled to the spin of the donor nucleus, $I \neq 0$ for all shallow donors in silicon. Thus the electron spin Hamiltonian in an applied magnetic field, B_0 , can be described to first order by $\hat{H} = g\beta B_0 S_Z + a S_Z I_Z$, where the first term is the Zeeman interaction, g is the electron g factor, β is the Bohr magneton, and the second term is the hyperfine interaction between electron and nuclear spins with hyperfine coupling constant, a , proportional to the electron

density at the impurity nucleus. The ¹²¹Sb donor examined in this work has $I = 5/2$ and therefore six possible resonant Zeeman transitions for electron spin: $\nu_{M_I} = (g\beta B_0 + aM_I)/h$, one for each projection, M_I , of the ¹²¹Sb nuclear spin, accounting for six absorption lines in the ESR spectrum of ¹²¹Sb [8].

Sample details were optimized for measurement with an X-band pulsed ESR spectrometer [9]. While an ideal Stark experiment would apply the same field to all donors via a parallel plate capacitor structure, ESR measurements require excitation of electron spins by microwaves, which tend to be shielded in the parallel plate arrangement. Therefore, interdigitated metal gates were lithographically patterned on the surface of a ²⁸Si epiwafer implanted with ¹²¹Sb at a dose of $4 \times 10^{11}/\text{cm}^2$ and mean implantation depth of 150 nm [Fig. 1(a)] [10]. The metal gate lines cover a large area for adequate ESR signal, have a short period to allow for large electric fields at small applied voltage bias, and are lengthwise and narrow to reduce absorption of the microwave electric field in the cylindrical ESR cavity. The device has 250 lines with 2.6 μm width at 14 μm period; overall dimensions of the interdigitated array are 19.5 mm by 3.5 mm. A 3 V bias between the interdigitated gates could be supported before the onset of an avalanche current. The interdigitated gates produce a dipolar electric field pattern across the implanted donors generating a distribution of field strengths shown in Fig. 1(b) [11]. In isotopically purified ²⁸Si the donor electron spin coherence is longer than in natural silicon, allowing for the long ESR pulse sequences described below. ¹²¹Sb donors were chosen instead of ³¹P in order to avoid a background ESR signal from unintended phosphorus impurities in the bulk and to better control the implantation depth.

Donor electron spin resonance Stark shifts cannot be detected with continuous wave (CW) ESR because Stark shifts are much smaller than the inhomogeneously broadened ESR linewidths: 0.2 MHz in isotopically purified ²⁸Si [4] and 6.7 MHz in natural silicon [12,13]. Therefore this work extends a pulsed ESR technique developed by Mims

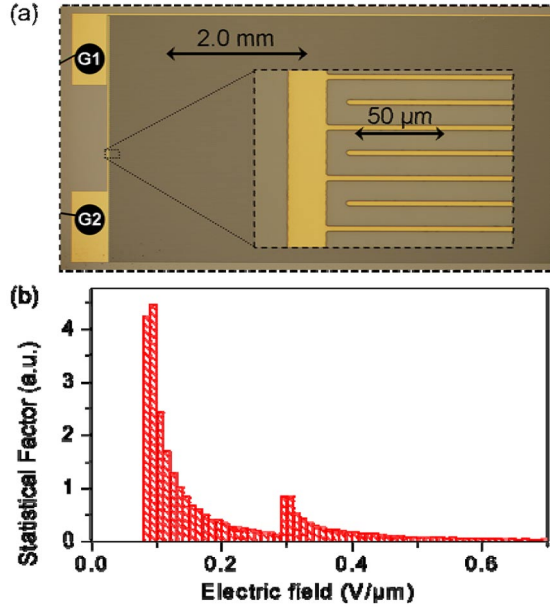


FIG. 1 (color online). (a) Micrographs of the interdigitated gate structure used in this work to measure the donor electron spin resonance Stark effect. Bonding pads for the two gates are labeled G1 and G2. Gate lines are oriented along a long side of the sample, a [100] axis. (b) Calculated electric field distribution at donor sites for 2 V applied between the interdigitated gates. Two peaks arise from the finite depth of the implanted antimony and the finite width of the gate lines.

[14] which is sensitive to small resonance shifts by integrating over time to accumulate measurable phase shifts in an echo signal. The basic pulsed ESR experiment, the two-pulse Hahn echo, is shown in Fig. 2(a). Two on-resonance microwave pulses with constant interpulse delay, τ , are used to generate a microwave echo signal. In addition, electrical pulses of varied strength, polarity, and timing are applied across the interdigitated gates. Figure 2(b) shows six electrical pulse sequences, referred to below as experiments I-VI. In the case of the regular Hahn echo experiment, i.e., no electrical pulse as in experiment I, the $\pi/2$ -pulse rotates spins into the plane normal to the applied magnetic field B_0 causing spins to precess. Spins precess at slightly different frequencies due to inhomogeneity in their local environment, and thus during the defocusing period the spin ensemble dephases. At time τ , the refocusing π -pulse reverses this dephasing trend by rotating spins through 180° . Since the individual spin precession frequencies are nearly invariant throughout the experiment, all spins are in phase again at time 2τ to generate an echo signal. The phase of the echo signal obtained in control experiment I is defined to be zero.

Electric field pulses applied during the spin echo experiment change the resonance (precession) frequencies of the electron spins via the Stark effect. In the case of a unipolar electrical pulse applied only during the defocusing period (experiment II) the spin echo signal acquires an additional,

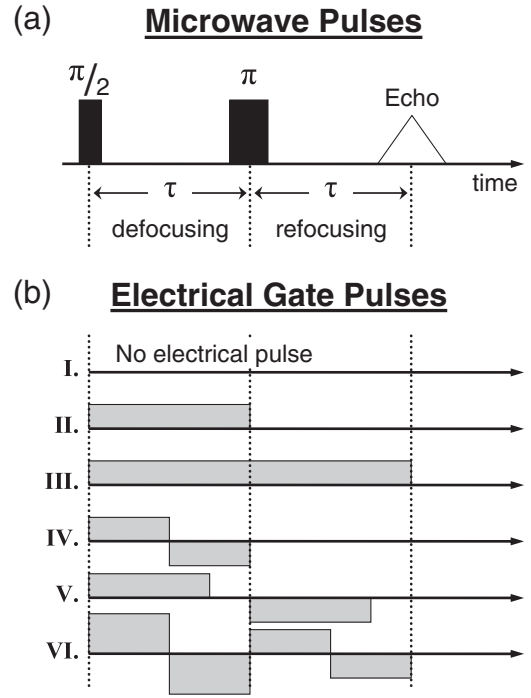


FIG. 2. Pulsed ESR sequences for measuring Stark effect in the $^{28}\text{Si}:\text{Sb}$ epilayer. (a) Two microwave pulses, with rotation angles $\pi/2$ and π and a constant interpulse delay τ , generate a Hahn echo signal at time 2τ . (b) Voltage pulses applied between gates G1 and G2 (Fig. 1) are time correlated with the microwave pulses.

uncompensated phase:

$$\varphi_{M_I} = \Delta\nu(E)\tau = [\Delta g(E)\beta B_0 + \Delta a(E)M_I]\tau/h, \quad (1)$$

where $\Delta\nu(E)$ is the Stark shift of the electron spin resonance frequency with individual terms for spin-orbit $\Delta g(E)$ and hyperfine $\Delta a(E)$ interactions. Experiment III is a control to verify that the Stark-induced phase shifts are fully refocused when a long uniform electrical pulse is applied to cover both defocusing and refocusing periods. In addition, we designed experiments IV and V with bipolar electrical pulses to resolve linear and quadratic Stark terms. First, by flipping the sign of the electric field midway through the τ period, precession phase shifts that depend asymmetrically on the field are refocused and only symmetric (quadratic) Stark shifts are accumulated with pulse sequence IV. Alternatively, in experiment V pulses of opposite polarity and equal duration are applied during the defocusing and refocusing periods which selectively detect only asymmetric (linear to lowest order) Stark shifts. The original pulse sequence by Mims (experiment II) accumulates phase shifts from both symmetric and asymmetric Stark terms. Experiment VI is a differential extension of experiment IV and is useful for measuring large phase shifts.

Figure 3 illustrates the spin echo phase shift observed using experiment IV. In this case, only quadratic Stark

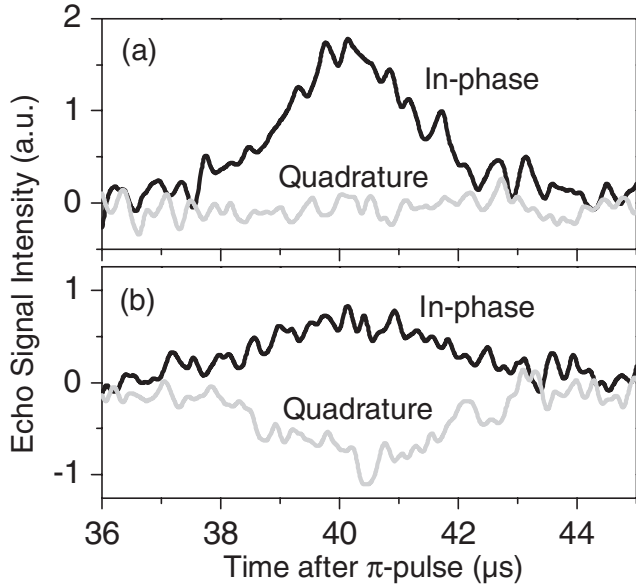


FIG. 3. Traces of the two-pulse (Hahn) echo signals measured on the $M_I = +1/2$ hyperfine line for $^{28}\text{Si}:\text{Sb}$ at 6.2 K and the interpulse delay $\tau = 40 \mu\text{s}$. In each plot the two signals represent the in-phase and quadrature channels of the microwave quadrature detector. (a) No gate voltage is applied (sequence I) and the detector is adjusted to produce a purely in-phase echo signal. (b) A bipolar pulse, $\pm 2 \text{ V}$, is applied (sequence IV) during the defocusing period, and the echo signal rephases with amplitudes in both the in-phase and quadrature channel, corresponding to a phase shift of 49° .

terms, $\Delta g(E) = \eta_g g E^2$ and $\Delta a(E) = \eta_a a E^2$, should be used in Eq. (1), with parameters η_g and η_a defining the strength of the Stark effects on the electron g factor and the hyperfine coupling constant, respectively. Because the interdigitated gate structure yields a distribution of electric fields at donor sites [Fig. 1(b)], the ensemble of donor electron spins experiences a distribution of Stark-induced phase shifts. We average over the calculated field distribution to model the phase and magnitude of the spin echo signal.

The main results of this work are summarized in Fig. 4 by plots of echo phase shifts versus voltage of the electrical pulses in experiment IV. Phase shifts are measured on four hyperfine lines in the ^{121}Sb spectrum, $M_I = \pm 1/2$ and $\pm 5/2$, allowing the estimation of individual contributions from the spin-orbit and hyperfine Stark effects. As seen in Eq. (1), phase shifts arising from the hyperfine Stark effect scale with M_I , whereas the spin-orbit Stark effect is equal for all lines. Thus, the observation of nearly equal and opposite phase shifts for lines $M_I = +5/2$ and $-5/2$ [Fig. 4(b)] shows that the hyperfine Stark effect dominates for these high M_I projections. The slight phase shift asymmetry observed for lines $M_I = +5/2$ and $-5/2$ is more pronounced for lines $M_I = +1/2$ and $-1/2$ [Fig. 4(a)], where the hyperfine shift is reduced by a factor of 5. This asymmetry shows that the spin-orbit and hyperfine Stark

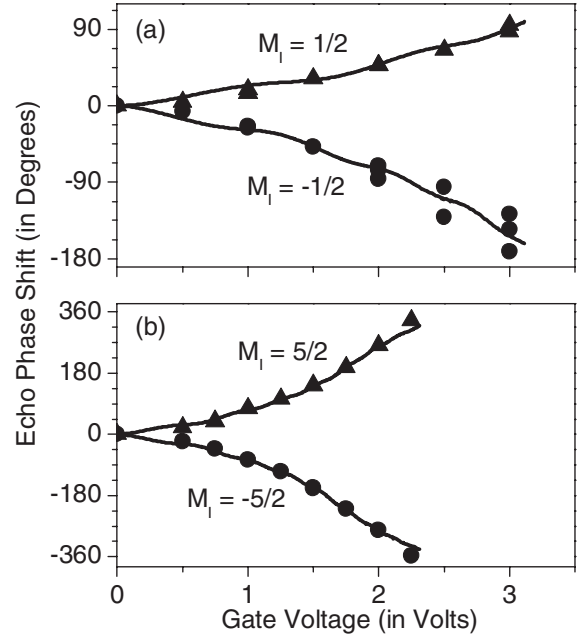


FIG. 4. Phase shift of the echo signal plotted as a function of the applied gate voltage for $^{28}\text{Si}:\text{Sb}$ at 6.2 K. Bipolar electrical pulse sequences IV and VI [Fig. 2(b)] were used with interpulse delay $\tau = 40 \mu\text{s}$. Data (points) and numerical fits (lines) are shown for the $M_I = \pm 1/2$ (a) and $M_I = \pm 5/2$ (b) hyperfine lines of the six line ESR spectrum of ^{121}Sb . Note that phase shifts for the $M_I = \pm 5/2$ lines are extended beyond 1.5 V with the differential voltage sequence (experiment VI). For the $M_I = -1/2$ line, the data in the 2–3 V range were obtained using both the standard bipolar (IV) and differential (VI) voltage sequences. The small oscillations in the calculated curves arise from the second, higher field peak in the electric field distribution [Fig. 1(b)].

shifts have the same sign and add constructively to produce a greater phase shift for $M_I = -5/2$ and $-1/2$, and the two effects tend to cancel each other resulting in a smaller phase shift for $M_I = +1/2$ and $+5/2$. From the signs of the echo phase shifts we deduce that the hyperfine Stark effect corresponds to a decrease in hyperfine coupling, a , and the spin-orbit Stark effect corresponds to a decrease in the electron g factor value. Fits for the four M_I projections shown in Fig. 4 are calculated using the same Stark hyperfine and spin-orbit parameters: $\eta_a = -3.7 \times 10^{-3}$ and $\eta_g = -1 \times 10^{-5}$ (in $\mu\text{m}^2/\text{V}^2$). In addition to electron spin resonance tuning, the hyperfine Stark parameter, η_a , also measures the spin resonance shift of the donor nucleus [1]. Repeated measurements establish an uncertainty of $\pm 10\%$ for hyperfine and $\pm 20\%$ for spin-orbit parameters.

Tetrahedral symmetry at the donor sites in silicon requires the Stark effects to be quadratic to lowest order. However, using electrical pulse sequence V we observed linear Stark effects evidenced by a decrease of echo magnitude with no shift in echo phase. These linear Stark effects imply asymmetries at individual donor sites with the average asymmetry over the donor distribution being

zero. We speculate that the asymmetries at donor sites arise from local strain fields which are probably dominated by the lattice mismatch between ^{28}Si and natural silicon with contributions from random defects. Lattice mismatch strain in ^{28}Si epiwafers similar to those used in this work has been evidenced in recent photoluminescence experiments [15] and strain in the silicon is known to shift the donor electron spin resonance [16]. Because of a lack of quantitative information about the sample's strain distribution, we do not attempt to quantify the observed linear Stark terms, but their existence suggests the importance of controlling strains for precise spin resonance tuning via the Stark effect.

The measured Stark parameters can be used to evaluate spin decoherence due to the Johnson noise in control gates of a Kane-like QC architecture. At an electric field which shifts the resonance by one linewidth ($\sim 1 \text{ V}/\mu\text{m}$), a 1 k Ω room temperature circuit resistance, and the donor embedded in a 0.1 μm thick Si layer between control gates, we calculate a decoherence time, T_2 (following Wellard and Hollenberg [17]), of over 10^3 seconds.

In conclusion, this study resolves two quadratic Stark effects for ^{121}Sb donors in silicon. The measured hyperfine Stark shift, $\eta_a = -3.7 \times 10^{-3} \mu\text{m}^2/\text{V}^2$, is smaller than that predicted for ^{31}P donors, $\eta_a = -2 \times 10^{-2} \mu\text{m}^2/\text{V}^2$ (as estimated from Fig. 2 in [6]). While calculations for ^{121}Sb donors and the spin-orbit term have not yet been done, one might expect η_a of ^{121}Sb to be comparable to or larger than η_a of ^{31}P , given the similar donor ionization energy and larger hyperfine coupling for Sb. More work will be needed to understand the differences between predicted and measured hyperfine shifts and to address the spin-orbit shift.

The ability to Stark tune the spin resonance is an integral and previously unmeasured parameter of Kane model donor spin QC architectures. Spin resonance shifts for ^{121}Sb donor electrons are found to be small at the moderate electric fields used in this work; a maximum shift of 25 kHz was observed when average electric fields of $\sim 0.1 \text{ V}/\mu\text{m}$ were applied with $M_I = \pm 5/2$. The hyperfine shift alone is enough to tune the ESR line about its width at a field of $1 \text{ V}/\mu\text{m}$, which is below the field at which calculations predict donor ionization [6] and possible to obtain if donor impact ionization is controlled by dilute doping and short intergate distances. Also, assuming η_g is independent of B_0 , the spin-orbit Stark effect will scale linearly with B_0 and will be the dominant shift mechanism at high magnetic fields, allowing for larger resonance shifts at lower electric fields. Alternatively, at specific magnetic fields and nuclear spin projections, e.g., $B_0 \approx 1.25 \text{ T}$ for $M_I = +1/2$, the hyperfine and spin-orbit Stark effects will cancel causing the electron spin resonance frequencies to be independent of electric field.

The authors would like to thank Igor Trofimov, Shyam Shankar, Rogerio de Sousa, Mark Friesen, Lloyd Hollenberg, and Cameron Wellard for helpful discussions. This research was supported at Princeton by the Army Research Office and the Advanced Research and Development Activity under Contract No. DAAD19-02-1-0040, and at Lawrence Berkeley National Labs by the National Security Agency under Army Research Office Contract No. MOD707501, the Department of Energy under Contract No. DE-AC02-05CH11231, and the National Science Foundation under Grant No. 0404208.

*Corresponding author.

Electronic address: bradbury@princeton.edu

- [1] B.E. Kane, *Nature (London)* **393**, 133 (1998).
- [2] R. Vrijen *et al.*, *Phys. Rev. A* **62**, 012306 (2000); T.D. Ladd *et al.*, *Phys. Rev. Lett.* **89**, 017901 (2002); A.J. Skinner, M.E. Davenport, and B.E. Kane, *Phys. Rev. Lett.* **90**, 087901 (2003); M. Friesen *et al.*, *Phys. Rev. B* **67**, 121301 (2003); R.G. Clark *et al.*, *Phil. Trans. R. Soc. A* **361**, 1451 (2003); S.J. Park *et al.*, *Microelectron. Eng.* **73-74**, 695 (2004).
- [3] J.P. Gordon and K.D. Bowers, *Phys. Rev. Lett.* **1**, 368 (1958).
- [4] A.M. Tyryshkin *et al.*, *Phys. Rev. B* **68**, 193207 (2003).
- [5] T.D. Ladd *et al.*, *Phys. Rev. B* **71**, 014401 (2005).
- [6] M. Friesen, *Phys. Rev. Lett.* **94**, 186403 (2005).
- [7] L.M. Kettle *et al.*, *Phys. Rev. B* **68**, 075317 (2003); M. Lu *et al.*, *J. Appl. Phys.* **98**, 093704 (2005); A.S. Martins, R.B. Capaz, and B. Koiller, *Phys. Rev. B* **69**, 085320 (2004); G.D.J. Smit *et al.*, *Phys. Rev. B* **70**, 035206 (2004); C.D. Hill *et al.*, *Phys. Rev. B* **72**, 045350 (2005).
- [8] R.C. Fletcher *et al.*, *Phys. Rev.* **95**, 844 (1954).
- [9] Pulsed ESR experiments were performed using an X-band spectrometer (Bruker Elexsys580) equipped with a helium cryostat (Oxford CF935). The temperature was set to 6.2 K, where the spin coherence time T_2 of Sb donor electrons is ~ 1 ms, which allows for long interpulse delays, τ , and long electrical pulses. Electrical pulses were generated using an arbitrary waveform generator (Agilent 33220A).
- [10] T. Schenkel *et al.*, *Appl. Phys. Lett.* **88**, 112101 (2006).
- [11] *FlexPDE, Finite Element Modeling Software* (PDE Solutions Inc., Antioch, CA, 2003).
- [12] G. Feher, *Phys. Rev.* **114**, 1219 (1959).
- [13] E. Abe *et al.*, *cond-mat/0512404*.
- [14] W.B. Mims, *Rev. Sci. Instrum.* **45**, 1583 (1974); W.B. Mims, *Phys. Rev.* **133**, A835 (1964).
- [15] A. Yang *et al.*, *Physica (Amsterdam)* **B376-377**, 54 (2006).
- [16] D.K. Wilson and G. Feher, *Phys. Rev.* **124**, 1068 (1961).
- [17] C.J. Wellard and L.C.L. Hollenberg, *J. Phys. D: Appl. Phys.* **35**, 2499 (2002).